Reviewed research article

Magnetostratigraphy, K-Ar dating and erosion history of the Hafrafell volcanics, SE–Iceland

Jóhann Helgason[1] and Robert A. Duncan[2,3]

[1]*National Land Survey of Iceland, Stillholti 14–16, 300 Akranes, Iceland*

[2]*College of Earth, Ocean, and Atmospheric Sciences, Oregon State University, Corvallis, OR 97331, USA*

[3]*Department of Geology and Geophysics, King Saud University, Riyadh, Saudi Arabia*

jhelgason@internet.is, rduncan@coas.oregonstate.edu

Abstract — *Glacial erosion in volcanic terrain just west of the Öræfajökull stratovolcano, SE Iceland, has carved >2-km-deep valleys. The ca. 2.8-km-thick stratigraphic sequence preserved in the mountain Hafrafell records evolution of landscape relief from relatively flat land at 4 Ma to a deeply dissected valley network today. Through geological mapping, magnetostratigraphy and K-Ar geochronology we establish that the area was first built up by lavas during the Gilbert chron, about 4 Ma. From about the same time we find the earliest evidence of glaciation. A 739-m-thick lava sequence formed, into which glaciers carved a ≥260-m-deep incision, the Hafrafell valley, during Matuyama time, >2 Ma. The incision was subsequently filled with lava flows during upper Matuyama time, <2 Ma. Mapping reveals 12 erosion surfaces, HR1–HR12, that formed during the last 4 Myr. The landscape evolution and erosion history of Hafrafell is divided into 6 stages with the first two occurring during the late Neogene, the Gilbert and Gauss magnetic chrons, when lava accumulation was slow and the landscape relatively flat. During stage 3, in lower Matuyama time, lava production increased by a factor of 2. During stage 4 the Hafrafell valley formed in upper Matuyama time. This stage marked clear development of more than 260-m-deep valleys. In stage 5 the Hafrafell valley was filled with subaerial and subglacial volcanic products. Finally, during Brunhes time, in stage 6, intense subglacial volcanism occurred near Hafrafell together with further valley network deepening to some 2-km-depth.*

INTRODUCTION

Volcanism and glacial erosion are two opposing factors that have shaped the landscape of Iceland since the Northern Hemisphere glaciation began. Central to unravelling this history is detailed mapping and dating of the stratigraphic record. Due to intense subglacial volcanism and its northerly location, Iceland's geologic record preserves information about climate change that can be traced well into the Neogene. Surrounding Öræfajökull stratovolcano in SE Iceland are Neogene to Quaternary volcanic strata that provide information about the onset of Earth's most recent sequence of glacial and inter-glacial intervals. The present day landscape is characterized by mountain "islands" located between glaciers and vast proglacial outwash plains. The bedrock consists mainly of lavas, sediments of various origins and sequences of subglacially erupted volcanics. Numerous active volcanoes continue to build positive topography while outlet glaciers from the Vatnajökull ice sheet actively erode and dissect the remaining volcanic massifs. In the Hafrafell mountain area, we trace the erosional evolution from a time when landscape was characterized by relatively flat lavas until the present state of deep valleys with abundant subglacial volcanism. Our study is based on detailed geological mapping, K-Ar age data, magnetostratigraphy and tracing of erosion surfaces within the stratigraphic sequence. Stud-

ies from different sites in Iceland have shown the first glaciations of the present ice age to extend back at least to 3–4 million years (Eiríksson and Geirsdóttir, 1996; Helgason and Duncan, 2001; Eiríksson, 2008; Geirsdóttir *et al.*, 2007). Refined correlation of these glacial events across the country awaits detailed work on high-resolution glacio-volcanic sequences such as those preserved in the Öræfi district due to deep erosion and volcanic accumulation in a rift flank zone.

RESEARCH AREA

The Hafrafell volcanic massif lies within the Öræfajökull Volcanic Zone (ÖVZ) that is located southeast of the accreting neovolcanic rift zone in NE Iceland (Figure 1). Crustal accretion in this area is minimal at present. Erosion, however, has exposed vast intrusions, both sheet swarms and major intrusive bodies (e.g. Walker, 1975). Hafrafell is located some 6 km west of the Öræfajökull stratovolcano and is enveloped between two southward-flowing glaciers, Skaftafellsjökull to the west and Svínafellsjökull to the east. Immediately north of Hafrafell, are the Hrútfjallstindar volcanic massif with a highest peak of about 1875 m. Hrútfjallstindar volcanics partly superimpose on the Hafrafell north end. The bulk of Hrútfjallstindar are stratigraphically younger than Hafrafell and formed during the Brunhes magnetic chron (< 0.781 Ma).

Previous work

Based on reconnaissance field work Prestvik (1979) suggested a broad division of Hafrafell into 6 units, the lowest being "basaltic lava flows with fine grained layers of sediments in-between. This unit, where alteration is most conspicuous, is frequently cut by basaltic dikes". Stratigraphically above, he defined two tillite beds and three units of "hyaloclastites and basaltic lava flows" with the top-most unit separated by an unconformity from "hyaloclastites and basaltic lava flows" below. Prestvik regarded the strata generally as basaltic but mentions a "silicic massif" higher up at Efri-Menn. Part of Prestvik's geochemical work included analyses of 5 dikes and lavas that he identified as tholeiite or dacite (Prestvik, 1985). On a geological map of SE Iceland, scale 1:250.000, Torfason (1985) presented a broad geological division of the Öræfi district in which he regarded all of Hafrafell's lower strata to be older than 3.1 Ma. For SE Iceland, Torfason's map shows widespread hyaloclastite formations of Quarternary age. Helgason and Duncan (2001) divided the stratigraphy of the Skaftafell area into glacial-interglacial stages (0–5 Ma) on basis of paleomagnetic work and K-Ar age dating. Helgason (2007) published a geological bedrock map of the Skaftafell area with detailed division of strata into rock formations, namely the Skaftafellsfjöll, Skaftafell, Hafrafell and Svínafell mountains. The present study is based on this mapping effort.

METHODS

Field mapping and stratigraphy

The Hafrafell massif (Figure 2) rises steeply from the sandur plain to the south, and is cut by a dike swarm that has led to numerous gullies with good exposure in the cliff section. Walker (1959) established a field classification scheme for the Neogene lavas of Eastern Iceland that we used during the mapping of Hafrafell (Figures 3 and 4). The basaltic lavas are defined either as (aphyric) tholeiite, (plagioclase) porphyritic or olivine basalt. However, the stratigraphic record includes frequent glacial-interglacial transitions with great volumes of subglacially formed strata. Thus, the geology of the area differs from typical Neogene lava terrains, as found in Eastern and Western Iceland, in the greater occurrence of subglacially erupted rocks, hyaloclastite horizons and evidence of erosion. The highly diversified lithology in Hafrafell required us to map numerous stratigraphic profiles. Based on correlations between profiles we divided the Hafrafell stratigraphy into 39 lithologic formations (HF1-HF39, Figure 4) that we then merged into eight groups, H1 to H8 (Figure 5). To constrain the time frame for stratigraphic evolution we sampled a master section for magnetic polarities and dated key units by the K-Ar method. Intercalated between lava flows are up to 30-m-thick hyaloclastite sedimentary units. We devide the brown hyaloclastite sediments into two types, namely "primary" and "laminated". The "primary" hyaloclastites typically massive, have

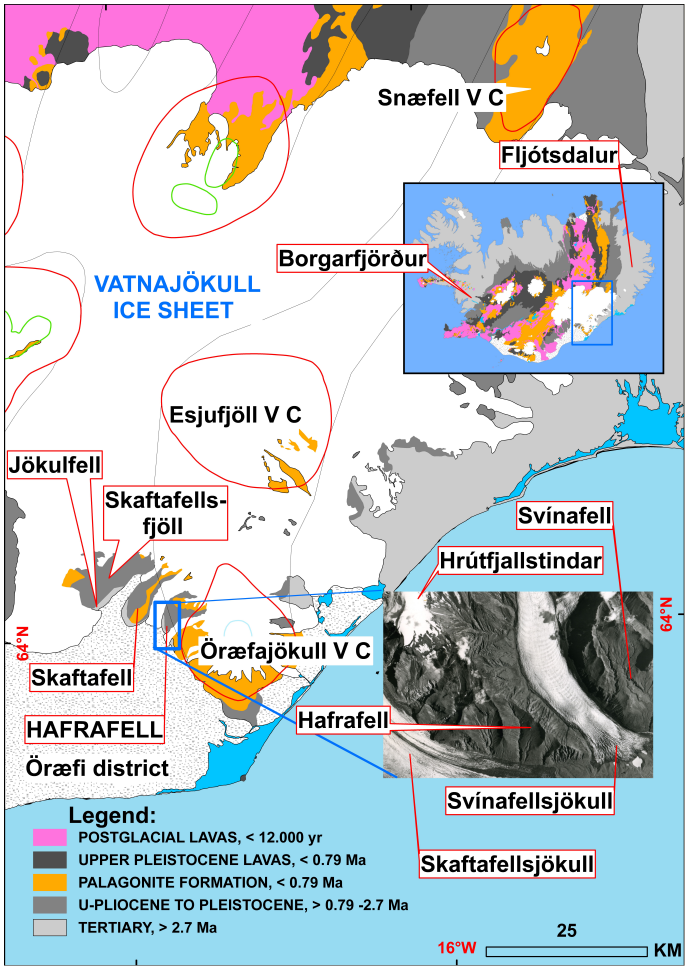

Figure 1. Geological setting of the Hafrafell research area (blue frame) in relation to the Öræfajökull volcano, neighboring volcanic centers (VC) east of the accreting rift zone. – *Jarðfræðilegar aðstæður Hafrafells (blár ferningur) í útjaðri megineldstöðvarinnar í Öræfajökli ásamt nærliggjandi megineldstöðvum fyrir austan rekbelti landsins.*

finely grained, brown hyaloclasite grains with dark gray to black, angular breccia fragments. We assume the primary hyaloclastite to have been rapidly transported to site of deposition and remained mainly intact thereafter. The laminated hyaloclastite is distinctly bedded with rounded to subrounded rocks, normally of variable lithology and color. We assume the laminated sediment to have been reworked and subjected to considerable transport from source. A total of 12 erosion surfaces, HR1 to HR12, were defined within the Hafrafell strata.

Dikes and alteration

Numerous near-vertical dikes cut through Hafrafell which, over a horizontal distance of some 1600 m, amounted to 234 m or 14.7% at 120 m a.s.l. Mean dike thickness is 2.5 m for 94 dikes. Mean dike strike is N70°E (22° s.d.). In addition a few near-horizontal dike sheets/sills are observed at the south end of Hafrafell. The intensity of dikes, sheets and rhyolite intrusions increases generally toward north. The south part of Hafrafell lies within the mesolite-scolecite zeolite zone but some 2 km farther north

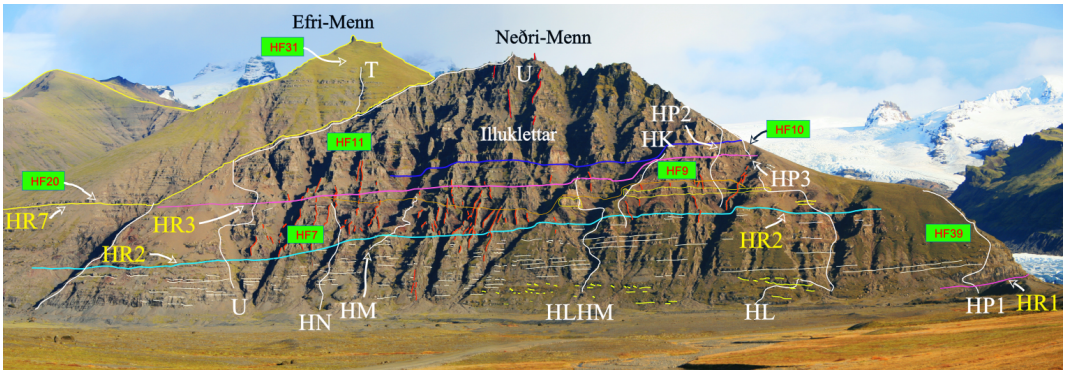

Figure 2. Hafrafell mountain viewed from west with the peaks of Efri-Menn (center) and Neðri-Menn further right. The Hrútfjallstindar peaks are seen behind Efri-Menn and the Öræfajökull volcano to the far right. Numerous gullies in Illuklettar, coincide with a dike swarm. Prominent dikes are shown in red. Stratigraphic profiles and some erosion surfaces and rock formations are also colored. Yellow lines near the base of Hafrafell, in sections HL and HLHM, indicate southward dipping lava lobe units. A blue line in Illuklettar, at the base of formation HF11, underlines a thick lava flow, unit HP32, that ponded at the onset of interglacial I5. Erosion horizons HR1 to HR3 are shown with pink and cyan lines. – *Hafrafell séð úr vestri, tinda Efri- og Neðri-Manna ber við himinn. Hrútfjallstindar sjást að baki Hafrafells en lengst til hægri gnæfa tindar eldstöðvarinnar í Öræfajökli. Fjölmörg gil í Illuklettum í Hafrafelli fara saman við gangasveim. Nokkrir áberandi berggangar eru merktir með rauðum línum. Jarðlagasnið ásamt upplýsingum um nokkra roffleti (HR) og myndanir (HF) eru einnig merkt á myndina. Gular línur nálægt neðri mörkum Hafrafells, í sniðum HL og HLHM, marka hraunalinsur með suðlægum halla. Blá lína í Illuklettum markar upphaf þykkrar hraunamyndunar HF11 á hlýskeiði I5, þar sem neðsta lagið, eining HP32, er óvenjuþykk vegna tjarnarmyndunar. Roffletir HR1 til HR3 eru sýndir með bleikum og ljósbláum línum.*

the lavas are within the laumontite zone where deeper crustal levels are exposed. Dikes in Hafrafell are typically of basalt composition (Prestvik, 1985).

Lava tilt and faults

Lava flows exposed at the southern part of Hafrafell dip gently about 1° toward N35°E but further north dip increases up to 20° toward the NW. High local dip values are associated with rhyolite intrusions exposed on Hafrafell's northeast side. Onyx banding in lava vesicles reveals progressive tilting. In one case within profile HAF (360 m a.s.l.) a tholeiite lava flow dips 18°/336° but a layered onyx amygdale dips only 7°/358°. Presumably, the intrusion of rhyolite caused the lava flow to dip 7° in addition to a previous dip of 11° (Walker, 1974). Two-stage dipping of layers, revealed in opal and onyx fillings, is not uncommon within lava flows on the north side of Hafrafell. On the NE side of Hafrafell (e.g. section HS) lava flows thicken toward the base of Hrútfjallstindar and increase in dip toward 45°. Faults are rare in Hafrafell but a few normal faults with a throw of up to 10 m were mapped. Faulting is not regarded a process that has influenced relief to any extent at Hafrafell.

Lava flow direction

Several cases are found in Hafrafell where lobes of lavas have flowed abruptly down slope. Although examples of such depositional dip are local they provide an indicator of past relief. The earliest case of this kind found in Hafrafell is at the base of section HL (Figure 6). Here lobes of a basaltic lava flow of formation HF3 interfinger with an underlying conglomerate or breccia with dip parameters 32°/202° suggesting a source slightly east of true north. Higher up in section HL, within formation HF9, lava lenses dip between 16–30°/165°, suggesting a lava source slightly west of true north. The steep depositional dips were only noted locally.

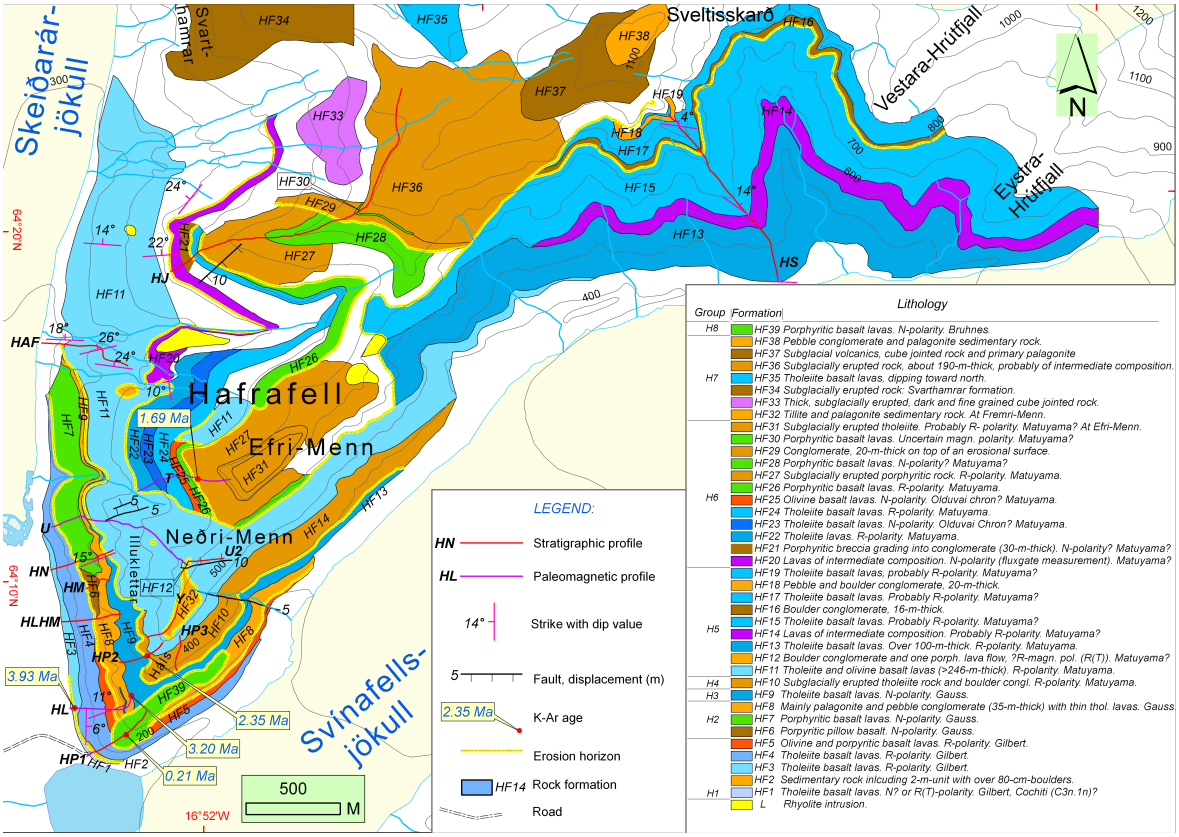

Figure 3. Detailed geological division of Hafrafell into formations (HF1–HF39) and groups. – *Berggrunnskort af Hafrafelli, greining jarðlaga í Hafrafelli í myndanir (HF1-HF39).*

Erosion surfaces in Hafrafell

A total of 12 erosion surfaces are defined for the Hafrafell section: HR1 to HR12 with stratigraphic location shown in Figures 3 and 4 and Table 1. The lowest surface, HR1, may record the onset of the ice age in SE Iceland. This lowest erosion surface is located in a quarry by the parking lot at the south tip of Hafrafell. The surface, HR1, is represented by a 12.5-m-thick sedimentary sequence that occurs between two tholeiite lava flows of formations HF1 and HF3 (Figure 4, profile HP1). Upward the sequence is divided into 6 units, A to F, (Figure 7).

Figure 4. Correlation of stratigraphic profiles in Hafrafell. Formation name, HF1 to HF39, appears next to each column, and erosion surfaces, HR1 to HR12, are indicated with red lines connecting through columns. Profile name, e.g. HL, HS or HAF, is provided at the top of each stratigraphic column. Age determinations appear next to dated units. Lava units drilled for paleomagnetic work are indicated with magnetic signature. Distances (m) between profiles are given at base of figure. – *Tenging milli jarðlagasniða í Hafrafelli. Heiti myndunar, HF1 til HF39, er sýnt til hliðar við hvert snið ásamt rofflötum, HR1 til HR12 sem tengjast með rauðum línum á milli sniða. Heiti sniðs er sýnt efst í sniði, t.d. HL, HS eða HAF. Aldur er sýndur til hliðar við aldursgreinda einingu. Segulstefna eininga er sýnd til hliðar við boraðar einingar vegna bergsegulmælinga. Fjarlægð á milli sniða (m) er sýnd neðst.*

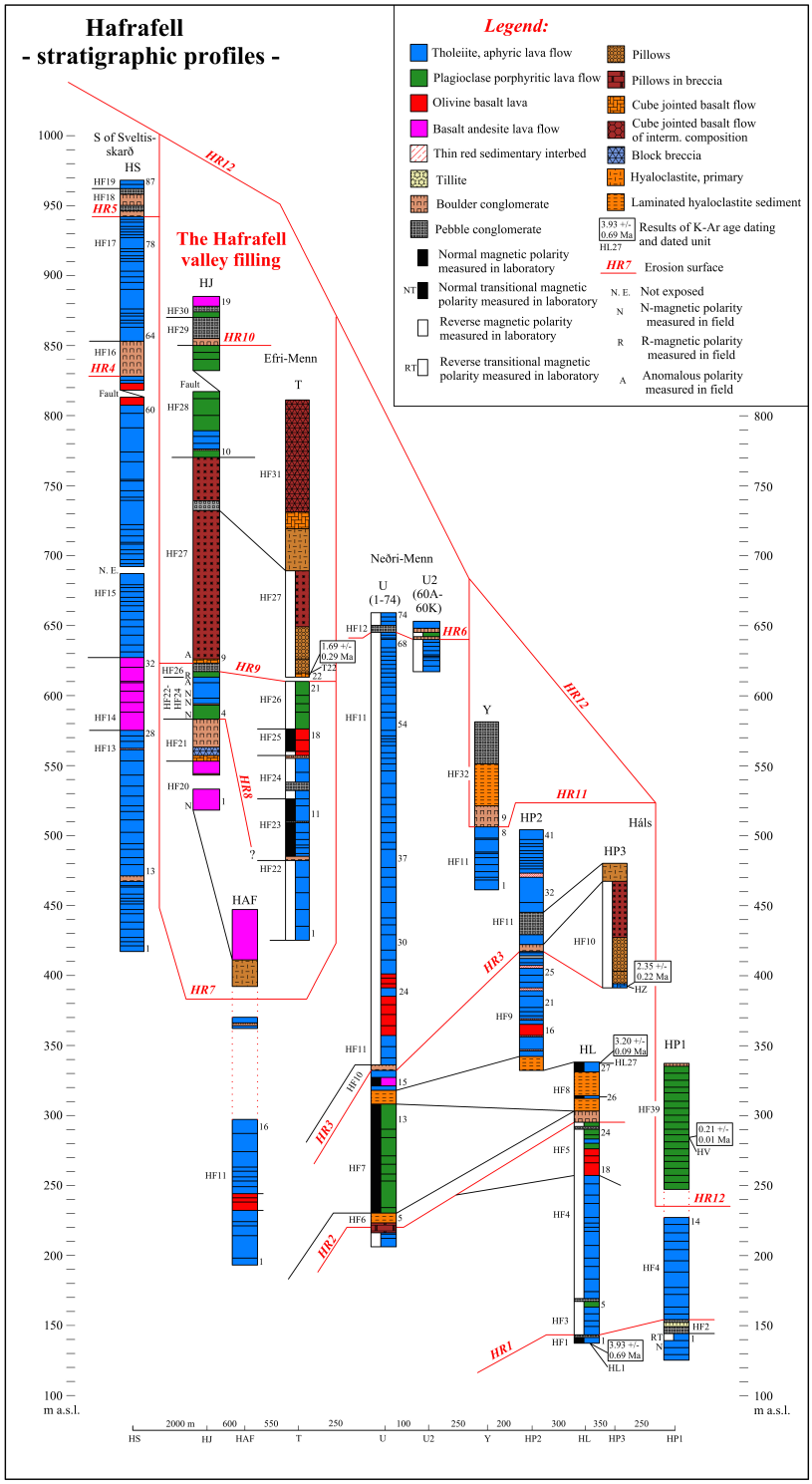
Hafrafell
- stratigraphic profiles -
Legend:
Tholeiite, aphyric lava flow
Plagioclase porphyritic lava flow
Olivine basalt lava
Basalt andesite lava flow
Thin red sedimentary interbed
Tillite
Boulder conglomerate
Pebble conglomerate
Normal magnetic polarity measured in laboratory
Normal transitional magnetic polarity measured in laboratory
Reverse magnetic polarity measured in laboratory
Reverse transitional magnetic polarity measured in laboratory
Pillows
Pillows in breccia
Cube jointed basalt flow
Cube jointed basalt flow of interm. composition
Block breccia
Hyaloclastite, primary
Laminated hyaloclastite sediment
Results of K-Ar age dating and dated unit
Erosion surface
Not exposed
N-magnetic polarity measured in field
R-magnetic polarity measured in field
Anomalous polarity measured in field
The Hafrafell valley filling
S of Sveltis-skarð
HS
HJ
HAF
T
Efri-Menn
Neðri-Menn
U (1-74)
U2 (60A-60K)
Y
HP2
HP3
HP1
HL
Háls
HR1
HR2
HR3
HR4
HR5
HR6
HR7
HR8
HR9
HR10
HR11
HR12
3.69 +/- 0.29 Ma
2.35 +/- 0.22 Ma
3.20 +/- 0.09 Ma
3.93 +/- 0.69 Ma
0.21 +/- 0.01 Ma
m a.s.l.
2000 m

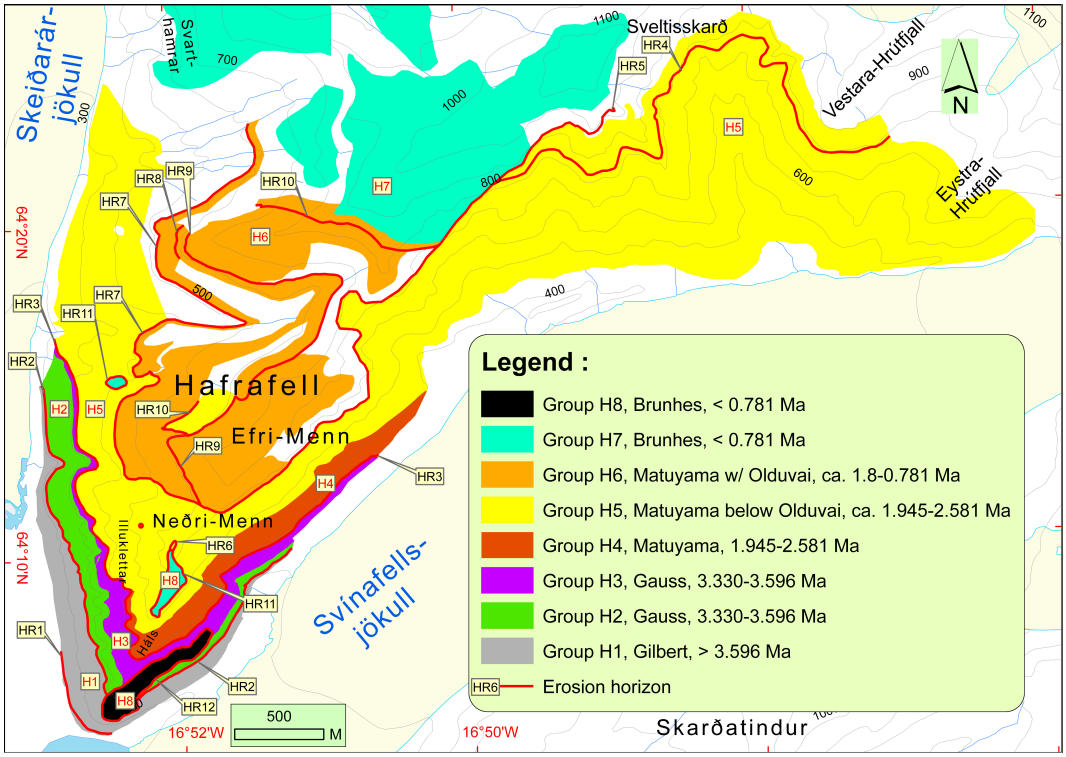

Figure 5. Broad stratigraphic division of Hafrafell showing groups H1–H8 with erosion surfaces HR1–HR12. – *Gróf skipting jarðlaga í Hafrafelli sýnir yfirmyndanir H1–H8 ásamt rofflötum HR1–HR12.*

In upper Hafrafell, marked by erosion surface HR7 (Figures 2, 3 and 4), are two contrasting sequences that occur side by side and extend from about 400 to 800 m a.s.l. They differ drastically in terms of lithology and magnetic signature. No faults are observed between them. One of them is rather fresh and not cut by dikes and has normal and reversely magnetized lavas, whereas the other is altered and cut by many dikes and has only reversely magnetized lavas. The younger sequence and less altered banks up against the other. This seems to us justifiable for invoking a valley into which lavas accumulated. Thus, fieldwork has established that here a valley was carved into the bedrock and one of these sequences, formations HF20–HF31, represents a filling of an ancient valley, henceforth referred to as the Hafrafell valley. The timing and extent of this valley filling is an important indicator for the erosion history by Hafrafell and probably elsewhere in Iceland.

Sampling for paleomagnetic measurements

Due to high dike density, especially within the lowest Hafrafell strata, it is locally difficult to measure magnetic polarity with a handheld magnetometer. To reliably establish magnetic polarity directions for the Hafrafell stratigraphic sequence we therefore sampled lava flows and pillow basalts to determine their magnetic polarity. We drilled a total of 104 volcanic units from 4 stratigraphic profiles in Hafrafell, namely sections HL, HP1, U and T. For each unit we drilled 4 samples with a portable two-stroke Pomeroy drill. Samples with core tube diameter of 2.5 cm and core length about 5 cm, were oriented in situ.

Rock demagnetization

We demagnetized cored samples at the rock magnetics laboratory at the Institute of Earth Sciences, University of Iceland, using Molspin alternating field demagnetization equipment. We measured magnetic di-

Figure 6. Lavas on top of the lowest sedimentary horizon have lenticular units that interfinger with underlying conglomerate/breccias. – *Hraunlög ofan á neðstu setmynduninni hafa linsulaga einingar sem fléttast saman við hnullungaberg/brekksíu fyrir neðan.*

rections in samples after peak field demagnetization steps of respectively 0, 10, 15 and 20 mT and best results chosen. Results were corrected for lava tilt of 1° toward N35°E.

Sampling for age determinations

Although the lowest exposed strata in Hafrafell are intensely cut by dikes, and within the mesolite-scolecite zeolite zone, we were able to find portions of flow units with low vesicle contents and surprisingly fresh interiors. In the upper sequence, lower grade zeolites are still abundant, but here we also collected relatively fresh samples, covering units ranging from oldest to youngest strata.

K-Ar analytical methods

We prepared groundmass separates from whole rocks for age determinations by crushing, sieving to obtain the 0.1–0.5 mm size fraction, ultrasonic washing in distilled water, drying and hand-picking under a binocular microscope to obtain the freshest, phenocryst-free samples possible, from 5 units with wide stratigraphic distribution. We loaded approximately 5 g of each sample into a Mo-crucible and a 1×10^{-8} vacuum was achieved by overnight baking (at 175°C) of the glass extraction line. Samples were then fused by radio-frequency induction heating of the crucible, and active gases gettered over a hot Ti–TiO_2 metal sponge. We then measured the isotopic composition of Ar mass spectrometrically using an AEI MS-10 instrument at Oregon State University, connected on-line with the gas extraction system. A known amount of ^{38}Ar (by calibration against standard FCT-3 biotite, 28.201±0.046 (Kuiper *et al.*, 2008) introduced during fusion to determine the concentration of radiogenic ^{40}Ar (Dalrymple and Lanphere, 1969). We made corrections for mass discrimination based on frequent measurements of atmospheric Ar from an on-line reservoir. K-contents were determined by atomic absorption spectrophotometry.

RESULTS

Paleomagnetic results

The magnetic polarity patterns for sections HL, HP1, U and T, together with information on polarity direction and VGP values are presented in Appendix 1. Magnetic polarity results are illustrated on the stratigraphic columns for Hafrafell (Figure 4). The results will be discussed below together with results of age determinations and stratigraphy.

Results of age determinations

Results of the K-Ar dating are given in Table 2, arranged in stratigraphic order. Stratigraphic height refers to position within the master section for Hafrafell. Formation number and coordinates further locate the stratigraphic position of each unit. Ages of dated units are also inserted on Figures 3 and 4. Analytical errors on total fusion ages (Ma) are reported

Table 1. Stratigraphy of Hafrafell. Division of rock formations into glacial and interglacial stages and their proposed correlation with the geomagnetic polarity time scale (Gradstein *et al.*, 2012). – *Jarðlagaskipan Hafrafells. Skipting jarðmyndana Hafrafells í jökulskeið og hlýskeið og ætluð tenging þeirra við segultímatal.*

Group no. and thickn.	Formation	Field classif. lithol.	Dip of strata[2]	Thickness (m)	Mag. pol.	Mag. chron	Mag. chron no.	Mag. age, Ma	^{40}Ar–^{39}Ar total fusion age, Myr	Inf. I-G stage	Er-surf.	Ref. Units[4]
H8 105 m	HF39	l, pl.ph	0°	105	N	Brunhes	C1n	<0.781	0.21±0.01 (HV)[1]	I12	HR12	HF14–HF33
	HF38	s, pebc		>130	N	Brunhes	C1n	<0.781		G	–	–
	HF37	sub, band		>160	N	Brunhes	C1n	<0.781		G	–	–
	HF36	sub, band		>190	N	Brunhes	C1n	<0.781		G	–	–
	HF35	l, th		>120	N	Brunhes	C1n	<0.781		I	–	–
	HF34	sub		180	N	Brunhes	C1n	<0.781		G	–	–
	HF33	sub		>140	N	Brunhes	C1n	<0.781		G	–	–
H7 995 m	HF32	s, till		75	–	Brunhes	C1n	<0.781		G	HR11	Y9–Y11
	HF31	sub, th		55	R?	Matuyama	C1r.2r	1.072–1.778		G11	HR10	T23
	HF30	l, pl.ph		5	R?	Matuyama	C1r.2r	1.072–1.778		I11	–	HJ18
	HF29	s, bcon		20	R?	Matuyama	C1r.2r	1.072–1.778		G10	HR9	HJ18/HJ17
	HF28	l, pl.ph		65	R?	Matuyama	C1r.2r	1.072–1.778		I10	–	HJ10–HJ17
	HF27	sub, pl.ph		74	R	Matuyama	C1r.2r	1.072–1.778	1.69±0.29 (T22)[1]	G9	–	T22
	HF26	l, pl.ph		34	R3	Matuyama	C1r.2r	1.072–1.778		I9	–	T19–T21
	HF25	l, olb		21	N3	Olduvai?	C2n	1.778–1.945		I9	–	T16–T18
	HF24	l, th		24	R3	Matuyama	C2r	1.945–2.581		I9	–	T13–T15
	HF23	l, th	15°/320°	25	N	Matuyama	C2n	1.945–2.581		I9	–	T6–T12
	HF22	l, th		60	R	Matuyama	C2r	1.945–2.581		I9	HR8	T1–T5
	HF21	sub, pl.ph		30	N?	Matuyama	??	1.945–2.581?		G8	–	HJ3
H6 448 m	HF20	l, band	10°/263°	35	N?	Matuyama	??	1.945–2.581?		I8	HR7	HJ1–HJ2
	HF19	l, th		>6	R?	Matuyama	C2r	1.945–2.581		I8	–	HS86–HS87
	HF18	s, bcon		20	–	Matuyama	C2r	1.945–2.581		G7	HR6	HS86/HS85
	HF17	l, th		90	R?	Matuyama	C2r	1.945–2.581		I7	–	HS64–HS85
	HF16	s, bcon		24	–	Matuyama	C2r	1.945–2.581		G6	HR5	HS64/HS63
	HF15	l, th	12°/35°	194	R?	Matuyama	C2r	1.945–2.581		I6	–	HS33–HS63
	HF14	l, band		51	R?	Matuyama	C2r	1.945–2.581		I6	–	HS29–HS32
	HF13	l, th		>100	R	Matuyama	C2r	1.945–2.581		I6	–	HS1–HS28
	HF12	s, bcon +1, pl.ph		8	R(T)	Matuyama	C2r	1.945–2.581		G5	HR4	U60K/U60I
H5 739 m	HF11	l, th		>246	R	Matuyama	C2r	1.945–2.581		I5	–	U28–U71
H4 90 m	HF10	sub, th		90	R	Matuyama	C2r	1.945–2.581	2.35±0.22 (HZ)[1]	G4	HR3	HZ
H3 78 m	HF9	l, th+band	10°/365°	78	N	Gauss	C2An	2.581–3.596		I4	–	HP2:14A–29
	HF8	s + l, th	20°/179°	37	N	Gauss	C2An	2.581–3.596	3.2±0.09 (HL27)[1]	G3?	–	HL27/HL26
	HF7	l, pl.ph	15°/338°	88	N	Gauss	C2An	2.581–3.596		I3	–	U5–U13
H2 156 m	HF6	sub, pl.ph	–	31	N	Gauss	C2An	2.581–3.596		G2	HR2	HM4–HM5
	HF5	l, olb + pl.ph		20	R	Gilbert	C2Ar	3.596–4.187		I2	–	HL18–HL25
	HF4	l, th	11°/340°	90	R	Gilbert	C2Ar	3.596–4.187		I2	–	HL6–HL17
	HF3	l, th + pl.ph		35	R	Gilbert	C2Ar	3.596–4.187		I2	–	HL2–HL5
	HF2	s, bcon+br		11	–	Gilbert	C2Ar	3.596–4.187		G1	HR1	HF1/HL0
H1 161 m	HF1	l, th		5	N or R(T)?[6]	Cochiti?	C3n.1n	4.187–4.300	3.92±0.06 (HL)[1]	I1	–	HL1 or HFX

Explanations: l: lava flow; s: sedimentary rock; th: tholeiite; band: basalt andesite; pl.ph: plagioclase porphyritic basalt; sub: rock formed under subglacial conditions; till: tillite; pebc: pebble conglomerate; bcon: boulder conglomerate; br: breccia; I: interglacial stage; G: glacial stage, N: normal magnetic polarity; R: reverse magnetic polarity; HR1 to HR12: erosional stages/surfaces. [1]Dated unit. [2]Dip and dip direction of strata. [3]R Magnetic polarity as measured with a handheld fluxgate magnetometer in the field. [4]Units of each formation that make up the composite stratigraphic column. [5]Dips toward north. [6]Weak N or transitional R.

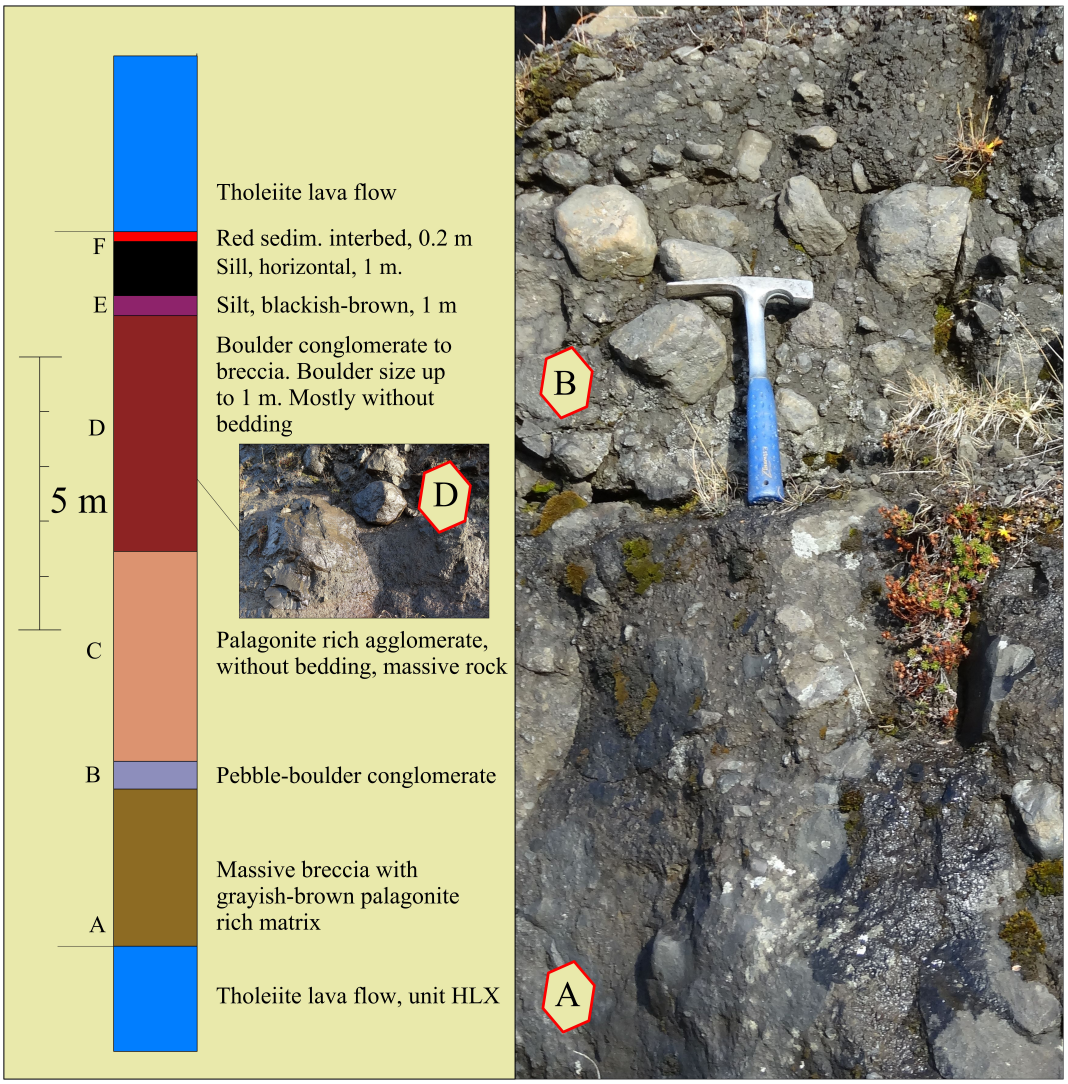

Figure 7. Erosion surface HR1. Left: The sedimentary horizon is divided into 6 units, A to F, that grade upward from massive breccia A, pebble-boulder conglomerate B, palagonite rich agglomerate C, boulder conglomerate or tillite D, silt E and thin red sand sized bed F. Units A and B are shown to the right. The lower unit A is a breccia with subrounded blocks embedded in hyaloclastite matrix. Upper unit B is a conglomerate with a softer matrix of sand and silt. Photo insert to the left shows unit D, a conglomerate or tillite with boulders up to 1 m in size. – *Rofflötur HR1. Sniðið til vinstri sýnir skiptingu setmyndunar í 6 einingar, A til F. Þær eru A: þétt breksía, B: völu- til hnullungaberg, C: móbergsríkt brotaberg, D: hnullungaberg eða jökulberg, E: silt og F: þunnt rautt sandsteinslag. Til hægri má sjá nánar einingar A og B þar sem eining er A massíf brekksía með lítt rúnnuðum hnullungum í brúnum glerkenndum grunnmassa en eining B hnullungaberg með grunnmassa af gráum sandi og silti. Innfellda myndin til vinstri sýnir einingu D með hnullungum allt að 1 m í þvermál.*

at the 2 standard deviation (95% confidence) level. These age determinations were originally reported in an appendix to Helgason and Duncan (2001). Here we present revised calculated ages in Table 2, using the decay and abundance constants recommended by Min *et al.* (2000) to conform with geologic time scale divisions of Gradstein *et al.* (2012).

DISCUSSION

Stratigraphic correlation with the geomagnetic time scale

We next correlate our results from K-Ar dating and paleomagnetic polarity determinations on Hafrafell units with the geomagnetic time scale (Gradstein *et al.*, 2012) as shown on Figure 8. The suggested correlation is based on data from profiles HL, HP1, HP3, U and T (Figures 4 and 9 and Table 2). The K-Ar age of each dated unit is shown at its stratigraphic position together with the stratigraphic position of erosion surfaces. The very lowest lavas sampled for paleomagnetic signature in section HP at the south end of Hafrafell (units HP1-1 and HLX) differ from the lavas next above in that one is normal while the other is R-transitional (shown as Nt on Figure 8). This suggests that the lavas at the very base of Hafrafell may belong to the Cochiti normal subchron (C3n.1n; 4.187–4.300 Myr). The lowest unit in section HL (Figure 4), that is normally magnetized, was dated at 3.92±0.06 Ma and correlates with the Cochiti normal sub-chron.

Next on top of unit HL1 begins a sequence with three main magnetic polarity intervals or upwards from R1-N1-R2 (Figure 8). The 829-m-thick R2-sequence has been dated near its base at 2.35±0.22 Ma (unit HZ), which identifies the R2-lava sequence as lower Matuyama (C2r; 1.945–2.581 Myr). Unit HZ, from an 85-m-thick subglacially erupted ridge, formation (HF10), generated relief. The first lava to bank up against it during the next interglacial stage showed clear lava ponding as is shown on Figure 2 with a blue line below a thick basalt lava flow beside formation HF10. The 234-m-thick N1-lava sequence below, for which we report an age of 3.20±0.09 Ma, is correlated with the Gauss interval (C2An; 2.581–3.596 Myr). The correlation suggests that the only part of Gauss time represented by Hafrafell strata is the N1 sequence that we correlate with C2An.3n (3.330–3.596 Ma). Unit HL27, in the upper part of N1 has an age of 3.20±0.09 Ma. Above dated unit HL27 in section HK are some 9 N-lavas (Figure 9). Thus lack of strata during Gauss in Hafrafell supports a hiatus during the period 2.581 to 3.330 Myr as suggested on Figure 8.

Higher up the section, in the Hafrafell valley filling, a number of reversals and brief magnetic events are recorded. Here the transitions are R2-N2-R3-N3-R4 (Figure 8). This sequence is older than Brunhes but presumably not far below the Brunhes/Matuyama boundary. A unit from R4 was dated at 1.69±0.29 Ma suggesting that the short N2 and N3 intervals correlate with the Olduvai subchron (1.778–1.945 Myr). Toward the top of the section all units are normally magnetized (N4), e.g. groups H7 and H8, and clearly of Brunhes age or younger than 781 kyr. The reported age of 215±12 ka for a lava flow from formation HF39 (group H8) allows this formation to be correlated with the third last interglacial (Mindel-Riss for the Alps; Holsteinian for N-Europe) and MIS 6 at about 191 ka (Gradstein *et al.*, 2012; Lisiecki and Raymo, 2005).

Stratigraphic division into groups H1 to H8

In order to trace the erosion history and landscape development at Hafrafell we have combined the 39 mapped rock formations into 8 groups (H1 to H8), from oldest to youngest. The distribution of the groups is presented in Figure 5 along with the 12 erosion surfaces, HR1–HR12. Of particular interest is the thick lava group, H5, into which a valley was incised, that probably represents an established valley network. We refer to this, at least 260-m-deep, depression as the Hafrafell valley. The valley sides consist of at least 739-m-thick lava sequence that formed during a relatively short interval, 1.945–2.581 Ma, or 0.64 Myr. The timing of the valley formation can be narrowed down to being older than the Olduvai subchron, as the stratigraphically lowest valley-infilling lavas are reversely magnetized and predate the Olduvai subchron. An age of 2 Ma would therefore be reasonable for the valley.

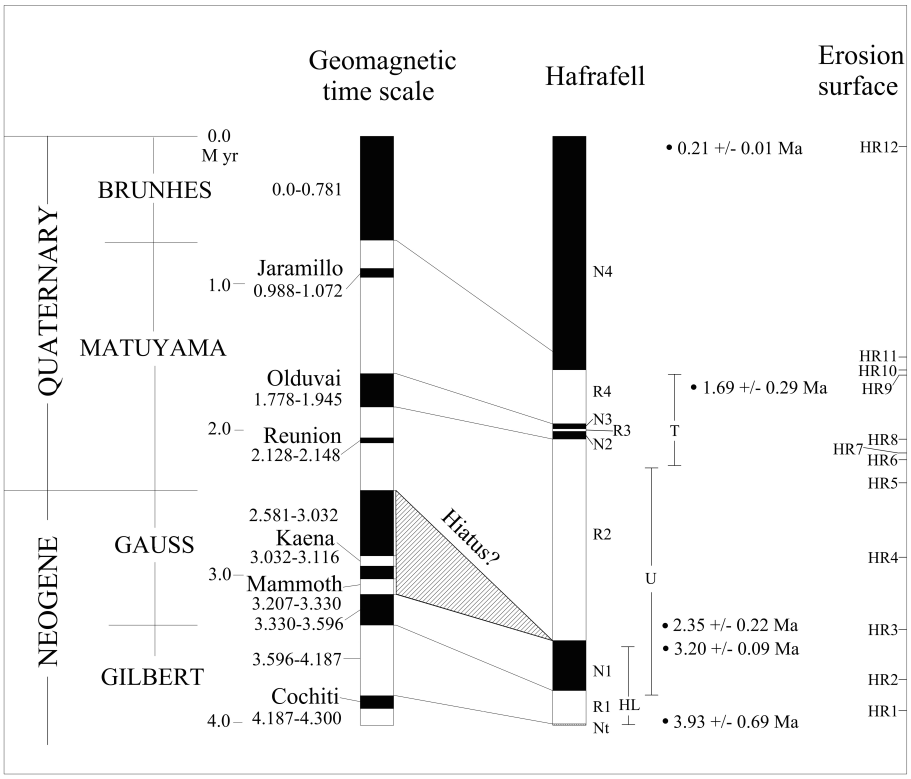

Figure 8. Correlation of the observed magnetostratigraphy from Hafrafell with the geomagnetic polarity time scale (Gradstein *et al.*, 2012). – *Tenging bergsegulstefnu Hafrafells við segultímatal.*

Table 2. K-Ar ages for selected stratigraphic units in Hafrafell. – *Niðurstöður aldursgreininga fyrir jarðlög Hafrafells.*

Sample no.	Coordinates	Stratigraphic height (m)	Total fusion age ±2sd (Ma)	%K rad.	%Ar rad.	Elevation m a.s.l.	Formation
HV	N64°0'32.76" W16°52'28.92"	2720	0.21±0.01	0.540	9.0	280	HF39
T22	N64°1'66.67" W16°51'59.03"	1496	1.69±0.29	0.158	2.8	616	HF31
HZ	N64°0'47.51" W16°52'7.68"	478	2.35±0.22	0.232	1.2	435	HF14
HL27	N64°0'42.83" W16°52'26.75"	298	3.20±0.09	0.299	12.5	340	HF8
HL1	N64°0'41.03" W16°52'48.71"	5	3.92±0.06	0.411	52.1	132	HF1

Ages calculated with the following decay and abundance constants: $\lambda_\varepsilon = 0.580\times10^{-10}$ yr^{-1}; $\lambda = 5.463\times10^{-10}$ yr^{-1}; ^{40}K/K = 1.17×10^{-4}.

Landscape evolution of SE Iceland

An intriguing question is how has the landscape of Iceland evolved from Neogene subaerial volcanism through some 20 glacials to a currently mountainous terrain with glaciers and deep valleys? Several studies have focused on the timing and frequency of glaciations in Iceland (e.g. Geirsdóttir, 2011). The timing of early valley formation and stratigraphic hiatuses presented in the current study may add details to this subject although it may remain speculative to what extent landscape evolution of SE Iceland has reflected

the whole of Iceland. With regard to the established stratigraphic framework for Hafrafell, erosion surfaces, valley formation, timing of events, stratigraphic correlation of magnetic chrons we now draw together the evolution though time (0-4 Ma) of erosion and volcanism in the area in six landscape stages (Table 3) as follows:

Stage 1. Volcanic strata in Hafrafell that predate the Gauss chron (> ca. 3.6 Ma) consist almost entirely of subaerially erupted lavas. We therefore conclude that erosion was minor (<50 m) with rivers acting as the dominant erosive agent.

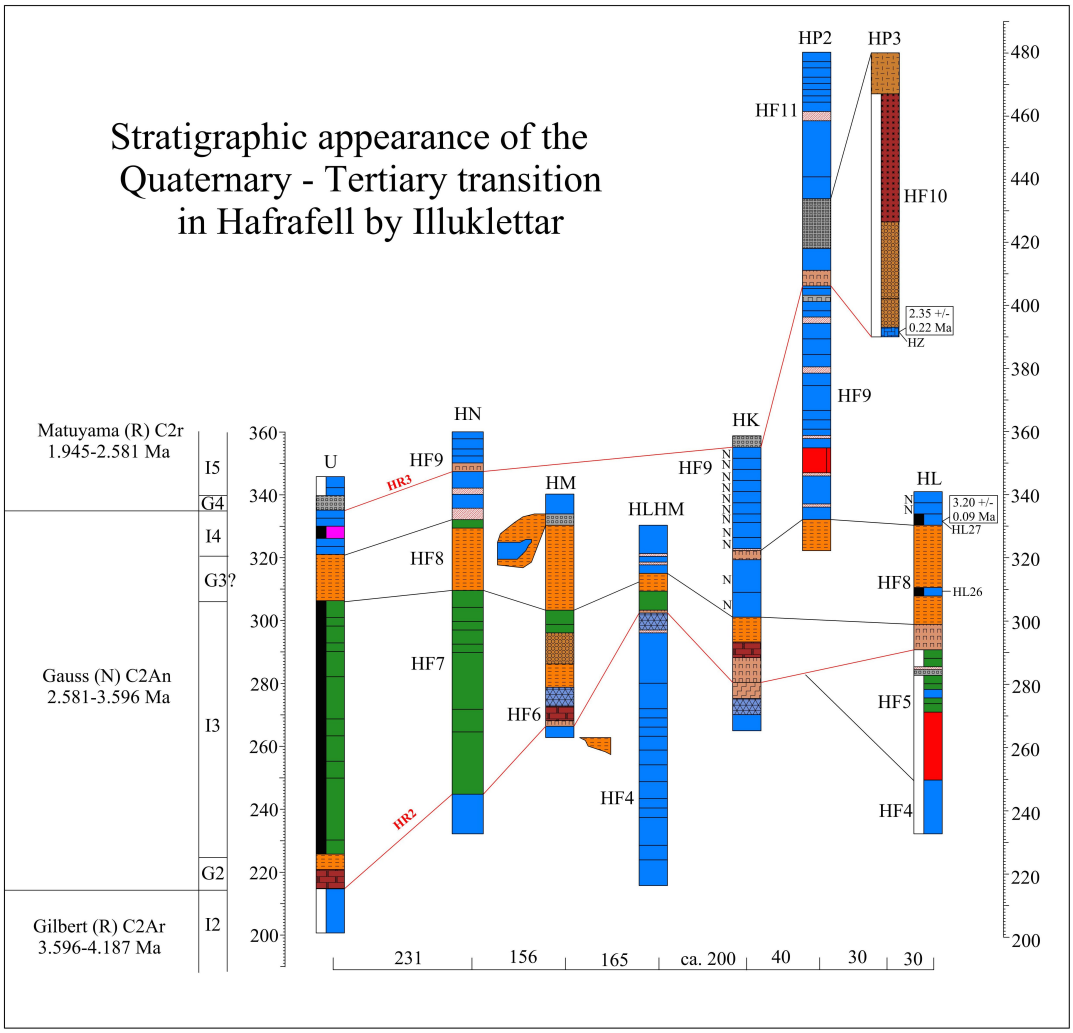

Figure 9. Appearance of glaciations in Illuklettar is here depicted with stratigraphic profiles from north (left) to south (right) extending upwards from Gilbert through Gauss to Matuyama chrons. Age and defined glacial- or inter-glacial division is shown on the left. Explanations as for Figure 4. – *Innkoma ísaldar í Illuklettum sýnd með jarðlagasniðum frá norðri (vinstri) til suðurs (hægri) sem ná frá segulmundum Gilbert (elst) upp í gegnum Gauss og Matuyama. Aldur og aðskilin hlýskeið/jökulskeið eru sýnd til vinstri. Skýringar eins og á 4. mynd.*

Table 3. Main stages in the landscape evolution of Hafrafell. – *Helstu stig í landslagsþróun Hafrafells.*

Land-scape stage	Erosion surface	Period / Chron	Age (Ma)	Group	For-mation	Thickness of volcanic strata (m)	Dominating activity	Relief[1] (m)
1st	HR1	Neogene Gilbert	4.187–3.596	H1	HF1–HF5	161	SAV2	+ 50?
2nd	HR2	Neogene Gauss	2.581–3.596	H2 + H3	HF6–HF9	234	SGV3	+ 100?
3rd	HR3–HR6	Quaternary Lower Matuyama	2.581–1.945	H4 + H5	HF10–HF19	829	SAV	>-829
4th	HR7	Quaternary Lower Matuyama		–	–	–	Erosion – Hafrafell	+ 260
			2.581–1.945	–	–	–	valley formation	
5th	HR8–HR10	Quaternary Upper Matuyama	1.945–0.781	H6	HF20–HF31	448	Hafrafell valley filled up, SAV + SGV	-448?
6th	HR11–HR12	Quaternary Brunhes	< 0.781	H7 +H8	HF32–HF39	1100	SGV	+1000

Explanations: [1]Relief: positive values indicate relief generation while negative values indicate landscape evening out due to accumulation. [2]SAV: Subaerial volcanism – lavas. [3]SGV: Subglacial volcanism – subglacially formed lithologies.

Stage 2. Subglacially erupted volcanics in Hafrafell date at least from the Gauss chron (ca. 2.6–3.6 Ma). Relief in Hafrafell during stage 2 is controlled by the sub-ice environment.

Stage 3. Volcanism during lower Matuyama (2.581–1.945 Ma) produced a $\geq$800-m-thick sequence of lavas, intercalated with a few erosion surfaces. This extensive volcanic activity in the Hafrafell area filled negative relief and smoothed landscape in relatively short time, $\leq$0.64 Myr.

Stage 4. During Upper Matuyama time, or from about the Olduvai subchron to almost the onset of Brunhes (ca. 1.945–0.781 Ma), older lava flow bedrock was carved by glacial erosion forming the >260-m-deep Hafrafell valley.

Stage 5. The Hafrafell valley was filled during Upper Matuyama time (ca. 1.945–0.781 Ma) with lava flows that contain the Olduvai subchron. The filling during this stage was a minimum of 260 m and may have been as much as 448 m.

Stage 6. During Brunhes time, volcanism was extensive from the Hrútfjallstindar and Öræfajökull volcanic centers (Helgason and Duncan, 2013; Stevenson *et al.*, 2006). Simultaneously, erosion continued and valleys deepened by at least 1000 m.

Topographic evolution

When considering the topographic evolution of eastern Iceland Walker (1982) stated: "the contrast between the Austfirðir and inland plateau is attributed to a departure about 5 m.y. ago from steady state conditions, caused by a significant southward migration of the locus of volcanism". This view does not consider the influence of glaciers on the landscape. We demonstrate that glaciers have generated over 2-km-deep valleys that formed roughly during the last 3.5 Myr at Hafrafell. We conclude that until about 3 Ma, glaciers had not set their mark on the region, either in the form of a valley network or formed the deep depression now present below the Vatnajökull ice sheet. Keeping in mind that SE Iceland is regarded a rift flank volcanic regime (Einarsson, 2008) it follows that subsidence of the volcanic products there should be much less than in the active accreting rift zones to the west and north. We speculate that the major intrusive process and lack of crustal subsidence is likely to generate local volcanoes that may reach high elevation above the surrounding area and actually higher elevation than comparable volcanic centers of the active rift zones. Also, the formation of inclined sheet swarms and major magma intrusion in SE Iceland has added to the crustal build-up (Walker, 1975). There, sheet intrusions commonly amount to over 50% of the stratigraphic sequence. Referring to the net movement caused by inclined sheets, Torfason (1979, p. 324) states: "the sheets and the major intrusions are the major cause of the extensive uplift of south-eastern Iceland, which is more than anywhere in Iceland."

These factors likely maintained the landscape in SE Iceland at relatively high elevation above sea level. Glacial erosion, on the other hand, may first have counteracted the positive build-up caused by rift flank volcanism and intrusions. Later, a deeply eroded valley system with high peaks in between would have

been characterized by nunataks with heights well above the pre-glacial level. The time-averaged effects of these processes may have governed elevation and relief of SE Iceland. As these factors are very different from the situation in the accreting volcanic rift zone the question arises: "how high was the land in the accreting rift zone compared to SE Iceland when an ice sheet first formed in Iceland?" This may be difficult to estimate. It may be argued, however, that during the Neogene, prior to major glaciations, the SE Iceland region was more elevated than the rest of Iceland as a result of the off-axis volcanic activity. We agree with Geirsdóttir (2011) who argues that an ice sheet first formed in SE Iceland and spread outward from there to the north and west.

A flexure zone was already present in SE Iceland in the late Neogene (e.g. Torfason, 1979; Klausen, 1999). This large-scale feature may possibly have contributed to the regional topography but we believe more detailed work is needed to conclusively evaluate its impact on Neogene landscape evolution.

The oldest tillite in Hafrafell

Based on the abundance of hyaloclastite and boulder conglomerates associated with the lowest erosion surface HR1 in Hafrafell, we conclude that it formed in response to glacial erosion. The age of HR1, about 4 million years, is almost the same as that of the tillite located at the base of Jökulfell (Thome, 1968; Helgason and Duncan, 2001; Helgason, 2007). The derived stratigraphic sequence there and radiometric age dating for the tillite, some 10 km west of Hafrafell (Helgason and Duncan, work in progress), suggests very similar age for both horizons. The similar age and stratigraphic location of these two outcrops suggests that the same glacial event formed the tillite at both sites. The importance of this tillite lies in its location and age that are in support of the idea that the earliest glaciations were confined to SE Iceland (Geirsdóttir, 2011). Further mapping of this horizon in SE and central E Iceland would therefore be valuable.

Gauss strata (Neogene-Quaternary transition) at Hafrafell

Near the end of the Gauss chron ($\sim$2.6 Ma), a thick sequence of hyaloclastite is found intercalated with lavas in Hafrafell. Erosion surfaces, HR2 and HR3 occur at the base and top of the Gauss strata, respectively. It is clear from Figure 9 that the strata from the Gauss normal polarity interval show a distinct north-south variation in lithology. On the north side sequence begins with highly plagioclase porphyritic lava flows in section U that grade up dip into similar composition pillow basalts some 400 m further south in section HM. On top of porphyritic formation HF7 are hyaloclastite sediments of formation HF8. Here tholeiite N-lavas (Gauss) inter-finger with the sediment in sections HM and HL (e.g. unit HL26), suggesting interglacial conditions in Hafrafell at this time. However, we conclude that the abundant hyaloclastite sediments associated with lava flows at this time means that glaciers were present further inland. Finally, a 70-m-thick sequence of tholeiite N-lavas overlies the sediments, being thickest at the southern tip of Hafrafell. There, steep but local depositional dips toward south are noted. Overall, the build-up of volcanic strata during Gauss time occurred through lenses of material added progressively at the southern end of Hafrafell.

Gauss-age strata in Hafrafell compared with Borgarfjörður and Fljótsdalur

Most magnetostratigraphic studies on Gauss-age rocks (2.581–3.596 Ma) in Iceland have been conducted on sequences that accumulated within accreting rift zones. Models of crustal accretion, such as that of Pálmason (1980), assume symmetrical build-up across the rift zones, with major subsidence and burial of erupted material at the rift axis. Following burial and spreading away from the rift zone, strata may eventually resurface due to erosion and uplift. In the Hafrafell rift flank region, however, the more voluminous lavas, or those that flowed greater distances from the rift zone axis, may preferentially be represented. Consequently, the exposed sections in Hafrafell are dominantly distal accumulations of the eruptive sequence. It is therefore interesting to compare results of the present study, from a rift flank region such as Hafrafell, with results from sequences originating in an accreting rift zone, namely from Borgarfjörður, W Iceland and Fljótsdalur, E Iceland (Figure 1).

Borgarfjörður. The Borgarfjörður sequence, W-Iceland is unique in its thorough recording of magnetic reversals where the study of McDougall *et al.* (1977) added the Þverá and Síðufjall subchrons to the geomagnetic time scale. The Gauss sequence in Borgarfjörður is about 435-m-thick but only 234-m-thick in Hafrafell. The Borgarfjörður sequence consists of subaerially erupted lava flows intercalated with 2 to 3 glacial horizons. In Borgarfjörður pillow basalts first occur well above Gauss or in strata with an age of about 1.6 Ma (McDougall *et al.*, 1977) wheras in Hafrafell the oldest pillow basalts have an age over 3.2 Myr. In the Borgarfjörður sequence the first 8 glacials have an age range of between 2.8 to 1.6 Myr and appear sharply intercalated between lava flows without any noticeable relief. In Hafrafell, strata belonging to Gauss time have a total thickness of only 234 m composed of: subaerially erupted lavas (169 m, 26 flows), sediments (34 m), and pillow basalts (31 m) with just two clear examples of glaciations and clear erosion surfaces that cut unconformably the underlying lava sequences.

What has caused the great difference in Gauss-age volcanic stratigraphy between these two regions? At least two factors could contribute to the observed differences, namely:

(a) *different accumulation rates (or volcanic production).* The comparison shows that the magnetostratigraphy in Borgarfjörður is more complete in containing a number of subchrons that are not present in Hafrafell, namely the reverse Kaena and Mammoth subchrons within Gauss in addition to the normal Jaramillo and Reunion subchrons of the Matuyama chron higher up in the composite section. This would suggest that even if intervals of intense erosion had occurred in Hafrafell, some remains of the subchron strata would still be present as erosion tends to be heterogeneous in valleys and thus leaving behind the valley walls. As this is not the case it is reasonable to conclude that the two times thicker Gauss section in Borgarfjörður is due to higher accumulation rates, being closer to a mature rift zone and more complete recording of the geomagnetic polarity time scale.

b) *axial rift zone versus rift flank environment.* The strata in Hafrafell (Figure 9) consist of lenses of lavas, sediments and breccias that are of much smaller dimensions, than seen at Borgarfjörður. There is a strong indication that strata in Hafrafell were built by progradational oblique lenses toward south during Gauss time. Clearly, considerable relief was present in Hafrafell while gentle lava plains with rivers and lakes appear to have characterized the Borgarfjörður section.

Considering these two factors we conclude that volcanic production/accumulation rates (McDougall *et al.*, 1977) were indeed much higher during Gauss time in Borgarfjörður than in Hafrafell. In Borgarfjörður the greater distance from the main ice sheet favoured greater preservation of the stratigraphic record compared to Hafrafell. Subsidence and burial within the accreting rift in Borgarfjörður also contributed to better preservation of the strata, a characteristic that did not apply to the Hafrafell region. Most likely, a large portion of the magmatic production in SE Iceland during Gauss time, and other intervals as well, formed intrusions (Walker, 1975) whereas in Borgarfjörður the magmas reached the surface and produced lavas.

The Gauss-age sequences in Hafrafell and Borgarfjörður both have glacial strata. At Hafrafell we observe a well-defined glacial deposit near the mountain base, of age close to $\sim$3.6 Ma. On the other hand the oldest glacial in Borgarfjörður is no older than $\sim$2.8 Myr. We note that for both areas only two to three glacials are found in the Gauss sequence. Three factors may explain the different stratigraphic thickness of the two Gauss sequences, namely that much greater erosion took place in the Hafrafell area that caused hiatuses there and smaller volcanic production caused slower accumulation rates. Thirdly, the early onset of glaciation in Hafrafell, at $\sim$3.60 Ma, compared with $\sim$2.80 Ma in Borgarfjörður, led to greater erosion during Gauss time in Hafrafell.

Fljótsdalur. Geirsdóttir *et al.* (2007) show five glacials during the Gauss magnetic chron in Fljótsdalur, E Iceland, some 120 km NNE of Hafrafell. Thus it is likely that glaciers there would simultaneously have occupied the Hafrafell area. However, the relatively thin stratigraphic Gauss sequence and associated erosion surfaces in Hafrafell, with only two

glacial intervals, may reflect that Hafrafell was centrally located at this time with regard to an ice sheet. In this case it may be that erosion in Hafrafell outweighed accumulation that lead to greater erosion and excess relief there during the Gauss chron. The greater erosion in Hafrafell may even have obliterated the evidence of at least 3 Gauss glacials that are present in the Fljótsdalur area relatively close by.

The Hafrafell dike swarm, age and possible source.

The Hafrafell stratigraphy and lava-dike relations do provide some information on the dike swarm age and source. Thus, we find the most likely source to be an old volcano that was active some 2 Ma and had a location near the Hrútfjöll area or in that direction with regard to Hafrafell. The dikes cut the top of Neðri-Menn, a lava sequence of Matuyama age. Below Neðri Menn, at 390 m a.s.l., we dated a lava flow at 2.35 Ma that therefore must be maximum age for the dike swarm. The swarm does not cut through the "Hafrafell valley strata", that are slightly older than Olduvai or 1.85 Ma. Most probably, the swarm was active at about 2 Ma or in the interval 1.85 to 2.35 Ma. The swarm trends into the Hrútfjöll lower sequence and the Hafrafell strata show "southward" building of lenses. The source for both the Hafrafell strata and dike swarm could therefore be in the general Hrútfjöll area.

SUMMARY AND CONCLUSIONS

The lowest strata in Hafrafell are lava flows that we correlate with the base of the Gilbert chron (C2Ar or 3.596–4.187 Ma), erupted at about 4 Ma. Upwards the lavas accumulated slowly during the Gilbert (C2Ar; 155-m-thick) and Gauss (C2An; 234-m-thick) magnetic chrons or during the interval 4.187–2.581 Ma. Dating and stratigraphic correlation suggests that during Gauss time strata accumulated only during early Gauss (C2An.3n or 3.330–3.596 Ma). Therefore, slow accumulation rates or more likely intensive erosion lasted through the onset of Matuyama chron (2.581–0.781 Ma) when a 739-m-thick sequence formed, predominantly of lavas.

We attribute slower accumulation rates in the Hafrafell lower sequence in part to its rift flank location, to the east of the axial rift zone. The Hafrafell lower strata accumulated through forward stacking of lenses that were added toward south or distally, as opposed to centrally constructed crust in the accreting rift zones. Twelve erosion surfaces, HR1 to HR12, are identified, based on tillite occurrences, subglacially erupted pillow basalts and glacially striated lava surfaces.

We divide the erosion and landscape evolution of Hafrafell into 6 stages. During the first two stages (late Neogene) volcanism was continuous but accumulation rates were slow and topographic relief was less than 100 m. During stage 3, i.e. lower Matuyama time, lava production increased and accumulation exceeded erosion. In stage 4, during upper Matuyama time, the Hafrafell valley formed and a valley network may have characterized the landscape. Stage 5, in upper Matuyama time, marked the filling up of the Hafrafell valley with lava flows and subglacial volcanics and evening out the established valleys. During stage 6, or the Brunhes chron, major subglacial volcanism took place with continuous erosion within $\sim$2-km-deep valley network.

Acknowledgements

The people of Freysnes and Svínafell in Öræfi are thanked for continued support over the years. We gratefully acknowledge the generous use of Leó Kristjánsson's laboratory, Institute of Earth Science, University of Iceland, for paleomagnetic measurements. *Friends of Vatnajökull*, a non-profit association of the Vatnajökull national park, is thanked for financial assistance to J.H. We thank Morten Riishus for many thought provoking comments on the manuscript. Critical review by David McGarvie on the manuscript led to significant improvements. An early part of this work was supported to J.H. by the Iceland Science Fund.

ÁGRIP

Jökulrof umhverfis eldstöðina í Öræfajökli, SA-landi, hefur grafið yfir 2 km djúpa dali. Þar, í Hafrafelli, bendir samsetning um 2.8 km þykks jarðlagasniðs til þess að landslag hafi þróast frá frekar flötu landi til mishæða og að lokum dalakerfa. Með kortlagningu

jarðlaga, ákvörðun bergsegulstefnu og aldursgreiningum sýnum við fram á að elstu hraunlög svæðisins mynduðust á Gilbert segulmund fyrir um 4 milljón árum síðan. Elstu ummerki jöklunar á svæðinu eru frá svipuðum tíma. Nokkru seinna, á neðri Matuyama, hlóðst upp 739 m þykkur stafli sem jöklar grófu "Hafrafellsdalinn"á Matuyama, fyrir meira en 2 milljón árum. Sú lægð fylltist af hraunlögum á efri Matuyama fyrir minna en 2 M árum. Kortlagning sýnir 12 rofstig, HR1–HR12, sem mynduðust á síðustu 4 milljón árum. Landmótun og rofsögu Hafrafells er skipt í 6 meginstig en tvö elstu urðu á Tertíer, þ.e. Gilbert og Gauss segulmundum, þegar upphleðsla hraunlaga var hæg og landslag tiltölulega flatt. Á stigi 3, neðri Matuyama, jókst hraunaframleiðsla um helming og kann landslag við Hafrafell að hafa jafnast mikið á þessum tíma. Í kjölfarið, á stigi 4, myndaðist „Hafrafellsdalurinn“ á efri Matuyama þegar að minnsta kosti 260 metra djúpur dalur varð til. Á stigi 5 fylltist „Hafrafellsdalurinn“ af hraunum og jökulgosbergi. Jarðlög dalfyllunnar hafa Olduvai segulmund sem sýnir að hún varð til á efri Matuyama (ca. 1.95–0.781 Ma). Á þessum tíma var dalakerfi til staðar. Á stigi 6, (Brunhes segulmund) varð mikil eldvirkni undir jökli umhverfis Hafrafell ásamt frekari dýpkun dalakerfis niður á allt að 2 km dýpi.

REFERENCES

Dalrymple, G. B. and M. A. Lanphere 1969. *Potassium-argon dating, principles, techniques, and applications to geochronology.* W.H. Freeman, San Francisco, 258 pp.

Einarsson, P. 2008. Plate boundaries, rifts and transforms in Iceland. *Jökull* 58, 35–58.

Eiríksson, J. 2008. Glaciation events in the Pliocene – Pleistocene volcanic succession of Iceland. *Jökull* 58, 315–329.

Eiríksson, J. and Á. Geirsdóttir 1996. A review of studies of the earliest glaciation of Iceland. *Terra Nova* 8, 400–414.

Geirsdóttir, Á. 2011, Pliocene and Pleistocene Glaciations of Iceland: A Brief Overview of the Glacial History. In: *Developments in Quaternary Sciences* 15, Ehlers, J. P. Philip, L. Gibbard and P. D. Hughes (eds.). Quaternary Glaciations "Extent and Chronology" A Closer Look, 199–210.

Geirsdóttir, Á., G. H. Miller and J. T. G. Andrews 2007. Glaciation, erosion and landscape evolution of Iceland. *J. Geodynamics* 43, 170–186. doi:10.1016/j.jog.2006.09.017.

Gradstein, F. M., J. G. Ogg, M. D. Schmitz and G. M. Ogg 2012. *The Geologic Time Scale 2012*, 2-Volume Set, (Oxford, U.K.), Elsevier, 1144 pp.

Helgason, J. 2007. *Bedrock geological map of Skaftafell, SE–Iceland, scale 1:25,000.* Ekra Geological Consulting.

Helgason, J. and R. A. Duncan 2001. Glacial–interglacial history of the Skaftafell region, southeast Iceland, 0–5 Ma. *Geology* 29, 179–182.

Helgason, J. and R. A. Duncan 2013. Stratigraphy, ^{40}Ar-^{39}Ar dating and erosional history of Svínafell, SE Iceland. *Jökull* 63, 33–53.

Klausen, M.B. 1999. *Structure of rift-related igneous systems and associated crustal flexures: examples from a Late Tertiary rift zone in SE Iceland and the Early Tertiary volcanic rifted margin in east Greenland.* PhD Thesis, University of Copenhagen, 283 pp.

Kuiper, K.F., A. Deino, F. J. Hiljen, W. Krijgsman, P. R. Renne and J. R. Wijbrans 2008. Synchronizing rock clocks. *Science* 320, 500–504.

Lisiecki, L. E. and M. E. Raymo 2005. Pliocene-Pleistocene stack of globally distributed benthic stable oxygen isotope records. doi:10.1594/PANGAEA.704257, Supplement to: Lisiecki, L. E., M. E. Raymo; A Pliocene-Pleistocene stack of 57 globally distributed benthic δ^{18}O records. *Paleoceanography* 20, PA1003, doi:10.1029/2004PA001071.

McDougall, I., K. Sæmundsson, H. Jóhannesson, N. D. Watkins and L. Kristjánsson 1977. Extension of the geomagnetic polarity time scale to 6.5 m.y.: K-Ar dating, geological and paleomagnetic study of a 3.500-m lava succession in western Iceland. *Geol. Soc. Am. Bull.* 88, 1–15.

Min, K., R. Mundil, P. R. Renne and K. R. Ludwig 2000. A test for systematic errors in ^{40}Ar-^{39}Ar geochronology through comparison with U/Pb analysis of a 1.1-Ga rhyolite. *Geochim. Cosmochim. Acta* 64, 73–98.

Pálmason, G. 1980. A continuum model of crustal generation in Iceland; kinematic aspects. *J. Geophys.* 47, 7–18.

Prestvik, T. 1979. *Geology of the Öræfi district, SE–Iceland.* Nordic Volcanological Institute, research report 7901, Reykjavík, 28 pp.

Prestvik, T. 1985. *Petrology of Quaternary volcanic rocks from Öræfi, southeast Iceland.* Rep. 21, Geol. Inst., NTH, Trondheim, 81 pp.

Stevenson, J. A., D. W. McGarvie, J. L. Smellie and J. S. Gilbert 2006. Subglacial and ice–contact volcanism at the Öræfajökull stratovolcano, Iceland. *Bull. Volcanol.* 68, 737–752. DOI 10.1007/s00445–005–0047–0.

Thome, K. N. 1968. Ein tertiärer(?) Tillit von Jokulfell am Sudostrand des Skeidarar-Gletschers in Island. *N. Jb. Geol. Paläont. Mh.* 7, 441–448.

Torfason, H. 1979. *Geological investigations into the structure of South-Eastern Iceland.* PhD thesis, University of Liverpool, 590 pp.

Torfason, H. 1985. *Geological map of Iceland, sheet 9, scale 1:250,000. SE–Iceland.* Icelandic Museum of Natural History and Iceland Geodetic Survey, Reykjavík.

Walker, G. P. L. 1959. Geology of the Reyðarfjörður area, eastern Iceland. *Quart. J. Geol. Soc. London* 114, 367–391.

Walker, G. P. L. 1974. The structure of Eastern Iceland. In: L. Kristjánsson ed. *Geodynamics of Iceland and the North Atlantic Area*, D. Reidel, 177–188.

Walker, G. P. L. 1975. Intrusive sheet swarms and the identity of Crustal Layer 3 in Iceland. *J. Geol. Soc. London* 131, 143–161.

Walker, G. P. L. 1982. Topographic evolution of Eastern Iceland. *Jökull* 32, 13–20.

Appendix I. Paleomagnetic results for Hafrafell, sections: HP, HL, U and T. – *Niðurstöður segulmælinga fyrir Hafrafell, snið HP1, HL, U og T.*

No	N	D	I	P_{Long}	P_{Lat}	α_{95}	J_{10}	Po
HP1-1	4	265.2	-59.4	237.0	-37.4	1.6	1.8	R(T)
HLX	3(2)	346.8	82.5	326.8	78.0	5.7	8.7	N
HL-1	4	203.4	-71.2	277.9	-75.8	6.5	3.6	R
HL-2	4	179.3	-67.2	345.3	-75.9	6.5	0.4	R
HL-3	4	203.1	-65.1	295.6	-69.0	10.3	0.3	R
HL-4	3(1)	188.1	-63.3	326.2	-70.3	8.5	3.4	R
HL-5	4	184.3	-64.1	333.9	-71.7	3.0	2.1	R
HL-6	4	194.1	-81.2	187.7	-79.9	3.4	3.3	R
HL-7	4	197.6	-64.9	305.6	-70.4	3.8	3.0	R
HL-8	4	205.7	-69.1	281.9	-72.6	4.1	4.1	R
HL-9	4	197.5	-65.2	305.3	-70.8	5.8	2.2	R
HL-10	4	198.3	-61.3	308.7	-66.0	5.8	3.4	R
HL-11	3(1)	185.5	-58.1	333.4	-64.6	5.3	2.6	R
HL-15	4	209.8	-37.5	304.4	-42.6	2.7	1.3	R(T)
HL-17	(4)							
HL-18	4	196.7	-73.6	275.8	-80.9	3.6	2.6	R
HL-19	3(1)	236.1	-68.9	248.9	-59.4	4.1	2.2	R
HL-20	3(1)	232.5	-84.4	188.9	-69.0	9.6	2.5	R
HL-21	4	163.6	-78.6	112.1	-82.2	2.5	2.1	R
HL-22	4	197.9	-73.0	277.4	-79.9	9.4	1.8	R
HL-23	4	199.8	-70.5	287.2	-76.4	2.9	1.5	R
HL-24	4	184.9	-73.3	316.0	-84.6	5.4	3.5	R
HL-25	3(1)	216.4	-59.6	284.1	-58.4	8.2	1.0	R
HL-26	4	321.2	74.9	263.4	72.4	4.5	1.5	N
HL-27	4	317.9	76.2	272.1	71.8	7.4	0.8	N
Hafrafell (U)								
U-1	4	280.1	-74.6	209.4	-48.6	8.8	2.4	R
U-2	3	216.0	-54.2	289.3	-53.5	9.4	0.6	R
U-7	3(1)	55.0	81.3	25.4	68.9	2.7	0.9	N
U-8	4	49.1	83.1	15.0	70.2	3.3	0.2	N
U-10	4	111.9	79.7	14.5	52.1	6.9	0.1	N
U-11	4	67.7	79.3	32.1	64.1	4.5	0.1	N
U-12	2	63.1	77.4	40.6	64.4	16.7	0.1	N
U-14	2(2)	183.0	-66.8	335.8	-75.3	2.1	1.6	R
U-17	4	234.1	-64.1	258.9	-55.4	4.7	1.2	R
U-20	4	213.6	-60.2	286.9	-60.0	3.2	3.4	R
U-21	4	219.1	-59.8	280.5	-57.5	2.2	6.2	R
U-22	4	221.6	-62.5	274.2	-59.2	2.3	3.7	R
U-23	4	207.9	-66.5	285.3	-68.9	3.2	1.7	R
U-24	2	225.0	-62.5	270.3	-57.8	4.3	4.8	R
U-25	3(1)	237.1	-67.2	251.3	-57.3	2.1	3.4	R
U-28	4	224.1	-70.1	256.7	-65.9	2.7	1.7	R
U-29	4	237.3	-69.7	246.3	-59.7	3.5	2.9	R
U-30	3	218.4	-73.9	248.4	-71.8	12.0	0.9	R
U-31	4	239.1	-62.6	256.1	-51.8	2.3	1.6	R
U-32	5	228.0	-64.8	263.8	-58.8	2.2	3.1	R
U-33	4	165.5	-56.7	8.5	-61.8	5.4	1.3	R
U-34	4	173.5	-61.1	356.3	-67.8	4.9	2.3	R
U-35	4	168.6	-58.2	4.1	-64.0	17.0	0.9	R
U-36	4	215.4	-63.6	280.2	-62.8	6.5	1.3	R
U-37	3(1)	122.6	-66.1	74.1	-56.0	32.8	0.2	R*
U-38	4	190.9	-82.1	178.7	-78.9	10.5	0.5	R
U-39	4	160.5	-72.4	48.7	-78.6	7.5	1.8	R
U-40	3(1)	192.2	-73.1	290.1	-82.1	8.1	1.3	R
U-41	4	193.0	-81.3	185.6	-79.9	2.9	5.8	R
U-42	5	222.4	-77.5	227.7	-72.4	14.2	1.1	R
U-43	4	140.1	-82.0	127.1	-73.0	6.8	2.6	R
U-44	4	126.6	-81.3	121.8	-69.4	2.2	3.2	R
U-45	4	138.2	-79.9	113.7	-73.0	2.9	3.5	R
U-46	3	164.2	-83.1	147.5	-76.6	17.1	1.7	R
U-47	4	192.1	-70.6	304.4	-79.0	10.9	1.3	R
U-49	3(1)	154.6	-71.6	54.0	-75.4	7.3	1.2	R
U-51	4	156.4	-78.8	108.9	-79.6	4.8	3.6	R
U-52	4	146.7	-75.4	82.6	-75.1	4.2	2.3	R
U-52A	4	136.4	-65.3	59.4	-61.2	13.3	0.9	R
U-53	4	143.6	-68.2	57.0	-67.3	7.8	0.8	R
U-54	4	166.8	-70.3	24.7	-78.4	7.7	3.0	R
U-55	4	153.8	-73.0	62.3	-76.4	3.8	1.5	R
U-56	3	151.9	-70.0	51.3	-72.6	3.9	3.4	R
U-57	2(2)	147.3	-76.1	86.6	-75.7	6.1	1.4	R
U-58	4	140.2	-73.0	75.7	-70.4	4.3	2.6	R
U-59	4	137.1	-70.0	68.8	-66.3	6.5	1.4	R
U-60	3	160.0	-79.3	115.8	-80.6	7.5	6.1	R
U-60A	4	153.3	-69.7	48.4	-72.9	5.9	5.5	R
U-60B	4	159.3	-63.4	24.8	-67.8	13.3	2.8	R
U-60C	4	159.0	-64.9	27.4	-69.3	8.8	2.1	R
U-66D	3(1)	162.6	-71.6	40.0	-78.5	5.5	2.3	R
U-60F	4	184.2	-65.2	333.7	-73.2	8.6	2.1	R
U-60G	2(1)	190.8	-69.8	310.5	-78.3	9.0	1.7	R
U-60H	4	189.9	-63.3	322.6	-70.0	12.5	1.3	R
U-60I	4	186.7	-66.3	326.9	-74.3	14.6	3.2	R
U-60J	2(2)	258.0	-45.0	251.6	-28.9	13.8	0.7	R(T)
U-60K	(4)							
Hafrafell (T)								
T1	4	206.2	-63.5	293.2	-66.1	3.2	5.6	R
T2	4	205.0	-63.0	295.8	-66.0	7.8	0.6	R
T3	4	208.3	-68.3	280.4	-70.7	10.1	3.4	R
T4	4	229.1	-64.9	262.6	-58.5	14.4	3.1	R
T5	4	237.9	-72.1	240.2	-61.8	9.0	1.2	R
T6	4	32.9	81.0	24.3	75.5	3.0	0.6	N
T7	4	9.0	78.7	20.1	84.4	12.9	0.8	N
T8	2(2)	333.9	68.8	224.8	72.1	29.2	0.3	N*
T9	4	124.6	82.9	3.5	54.2	3.5	4.7	N
T10	4	353.8	43.7	172.4	51.3	18.2	3.2	N
T11	4	357.5	63.5	169.0	71.0	11.0	0.7	N
T12	4	11.6	71.9	119.9	80.9	18.9	0.9	N
T13	3(1)	228.6	-52.9	275.6	-47.6	14.7	1.2	R
T14	2(2)	236.1	-67.1	252.3	-57.6	1.5	2.1	R
T15	4	221.2	-63.9	272.7	-60.8	2.0	9.6	R
T16	4	342.3	-74.5	173.9	-35.7	17.3	1.0	R(T)
T17	3(1)	47.7	82.5	18.2	70.8	7.4	1.2	N
T18	3(1)	14.9	80.4	14.9	80.8	26.2	0.3	N*
T19	3(1)	195.9	-62.5	311.9	-67.9	2.7	3.8	R
T20	3(1)	188.4	-81.9	176.1	-79.4	6.1	4.2	R
T21	4	213.4	-85.1	180.4	-71.4	5.1	9.8	R
T22	4	199.6	-65.1	301.6	-70.0	11.6	3.1	R

Explanations: No: Unit number. N: Number of measured samples with number of rejected samples in brackets. D, I: Declination and inclination after tilt correction. P_{Long}: Longitude of virtual geomagnetic pole (VGP). P_{Lat}: Latitude of virtual geomagnetic pole (VGP). α_{95}: Mean field 95% confidence radius. J_{10}: Remanence intensity (Amperes/m) after demagnetization in 10 mT AF. N: Normal polarity. R: Reverse polarity. (T) Transitional.